NIH Public Access
Author Manuscript
J Bone Miner Res. Author manuscript; available in PMC 2007 August 2.

Published in final edited form as:
J Bone Miner Res. 2006 October ; 21(10): 1657–1665.

$\alpha_9\beta_1$: A Novel Osteoclast Integrin That Regulates Osteoclast Formation and Function

Hongwei Rao[1], **Ganwei Lu**[1], **Hiroshi Kajiya**[2], **Veronica Garcia-Palacios**[1], **Noriyoshi Kurihara**[1], **Judy Anderson**[1], **Ken Patrene**[1], **Dean Sheppard**[3], **Harry C Blair**[4], **Jolene J Windle**[5], **Sun Jin Choi**[6], and **G David Roodman**[1,7]

1 *Medicine-Hematology/Oncology, University of Pittsburgh, Pittsburgh, Pennsylvania, USA*

2 *Fukuoka Dental College, Sawara-ku, Fukuoka, Japan*

3 *Department of Medicine, University of California at San Francisco, San Francisco, California, USA*

4 *Department of Pathology, University of Pittsburgh, Pittsburgh, Pennsylvania, USA*

5 *Department of Human Genetics, Virginia Commonwealth University, Richmond, Virginia, USA*

6 *National Institute of Dental and Craniofacial Research, Bethesda, Maryland, USA*

7 *Medicine-Hem/Onc, VA Pittsburgh Healthcare System, Pittsburgh, Pennsylvania, USA*

Abstract

We identified a previously unknown integrin, $\alpha_9\beta_1$, on OCLs and their precursors. Antibody to α_9 inhibited OCL formation in human marrow cultures, and OCLs from α_9 knockout mice had a defect in actin ring reorganization and an impaired bone resorption capacity.

Introduction— Integrins play important roles in osteoclast (OCL) formation and function. Mature OCLs mainly express $\alpha_v\beta_3$ integrin, a heterodimer adhesion receptor that has been implicated in osteoclastic bone resorption. We identified ADAM8, a disintegrin and metalloproteinase, as a novel stimulator of OCL differentiation and showed that the disintegrin domain of ADAM8 mediated its effects on OCL formation. Because the disintegrin domain of ADAM8 does not bind Arg-Gly-Asp (RGD) sequences, we determined which integrin bound ADAM8 and characterized its role in OCL formation and activity.

Materials and Methods— Chinese hamster ovary cells (CHO) expressing different integrin subunits were tested for their capacity to bind the disintegrin domain of ADAM8. Mouse or human bone marrow cells and purified OCL precursors were tested for $\alpha_9\beta_1$ integrin expression by Western blot, immunocytochemistry, and real-time RT-PCR. A monoclonal antibody to human α_9 was used to block $\alpha_9\beta_1$ on OCL precursors stimulated by 1α,25-dihydroxyvitamin D_3 [1α,25$(OH)_2D_3$] or RANKL. Vertebrae of 7-day-old $\alpha_9^{-/-}$ mice and wildtype (WT) littermates were compared using bone histomorphometry and 3D μCT analysis.

Results— α_9 integrin was expressed by mouse and human bone marrow–derived OCLs and their precursors. Importantly, the anti-α_9 antibody inhibited human OCL formation stimulated by 1α,25$(OH)_2D_3$ or RANKL dose-dependently. Furthermore, analysis of OCLs formed in marrow cultures from $\alpha_9^{-/-}$ mice showed that the OCLs formed were more contracted and formed significantly less bone resorption pits on dentin slices. Histologic analysis of $\alpha_9^{-/-}$ vertebrae showed thickened trabecular regions and retained cartilage within vertebral bodies of $\alpha_9^{-/-}$ mice. 3D μCT analysis of

Address reprint requests to: G David Roodman, MD, PhD, VA Pittsburgh Healthcare System, R&D 151C-U, Room 2E-113, University Drive, Pittsburgh, PA, 15240, USA, E-mail: roodmangd@upmc.edu

Dr Roodman received corporate appointments from Amgen, Merck & Co., Millennium, Novartis, and Scios, and he has received funding from Celgene. All other authors state that they have no conflicts of interest.

$\alpha_9^{-/-}$ vertebrae also showed a significant increase in trabecular bone volume/total tissue volume and a tendency for decreased trabecular separation compared with WT mice.

Conclusions— These results support a previously unknown role for $\alpha_9\beta_1$ integrin in OCL formation and function.

Keywords

$\alpha_9\beta_1$ integrin; osteoclast; ADAM8; α_9 knockout mice

INTRODUCTION

Osteoclasts (OCLs) are multinucleated cells formed by the fusion of precursors in the monocyte/macrophage lineage.(1,2) OCL formation and function involve a series of developmental and regulatory steps including homing to bone by hematopoietic progenitor cells, migration of OCL precursors to the area of bone to be remodeled, cell proliferation, attachment of OCL progenitors to the bone, and fusion of mononuclear precursors to form multinucleated OCLs that are activated and resorb bone. Many of these steps involve cell–cell and cell–matrix adhesion. Several factors affect osteoclastogenesis at different stages of development, including 1α,25-dihydroxy-vitamin D_3 [1α,25$(OH)_2D_3$], RANKL, macrophage-colony-stimulating factor (M-CSF), interleukin-1 (IL-1), TGF-β, TNF-α, IL-6, and PTH.(1) In addition, several autocrine/paracrine factors are produced by OCLs that regulate OCL formation and activity.(3–5)

ADAM8, a member of the ADAM gene family, is an autocrine factor expressed by OCLs that is involved in the later stages of OCL formation.(6) The ADAM family is comprised of proteins that have transmembrane and cytoplasmic domains containing metalloproteinase (MMP)-like, disintegrin-like, cysteine-rich, and epidermal growth factor (EGF)-like domains. ADAM family members have been implicated in cell fusion and cell-to-matrix adhesion(5,7) and can act as signaling molecules. These functions are vital for normal cellular processes such as cell morphogenesis, wound healing, tumor cell invasion, and metastases.(8,9) ADAM8 is expressed primarily in cells of the monocyte/macrophage lineage as a type 1 membrane–anchored protein.(10) We previously reported that the disintegrin domain of ADAM8 mediated its stimulatory effects on OCL formation.(6) However, the integrin mediating the effects of ADAM8 on OCL formation had not been previously identified. $\alpha_v\beta_3$ is abundantly expressed by OCLs, and specifically binds to the Arg-Gly-Asp (RGD) domain. $\alpha_v\beta_3$ plays an important role in the resorptive process.(11) OCLs also express other integrins at lower levels, such as $\alpha_2\beta_1$, $\alpha_v\beta_1$, $\alpha_v\beta_5$, and $\alpha_5\beta_1$. (12) ADAM8 lacks an RGD motif and has the RX_6DLPEF sequence, which is an $\alpha_9\beta_1$ recognition motif. This study shows that $\alpha_9\beta_1$ integrin is expressed on OCLs and their precursors and that $\alpha_9\beta_1$ integrin is the receptor for ADAM8 that mediates its effects on osteoclastogenesis. Furthermore, we show that OCLs lacking α_9 have an abnormal cytoskeleton and a decreased bone resorption capacity.

MATERIALS AND METHODS

Reagents and antibodies

RANKL (Amgen, Seattle, WA, USA) and 1α,25$(OH)_2D_3$ (Teijin, Tokyo, Japan) were generously provided for these experiments. Recombinant human M-CSF was purchased from R&D Systems (Minneapolis, MN, USA). Restriction enzymes, *Taq* DNA polymerase, FCS, and tissue culture media were purchased from Invitrogen (Grand Island, NY, USA). Mouse anti-human $\alpha_9\beta_1$ monoclonal antibody was purchased from US Biological (Swampscott, MA, USA). The polyclonal antibody against murine α_9 was generously provided by Dr Dean

Sheppard (University of California at San Francisco), and all other chemicals were obtained from Sigma (St Louis, MO, USA).

Animals

Four- to 6-week-old C57BL/6 mice were obtained from Jackson Laboratories (Bar Harbor, ME, USA). α_9 heterozygote mice were generously provided by Dr Dean Shep-pard(13) and bred under conditions approved by the IACUC at Virginia Commonwealth University. Seven-day-old $\alpha_9^{-/-}$ mice were used for cell culture, μCT, and histologic studies.

Adhesion assays

Adhesion assays were performed as reported by Eto et al.(14) Briefly, 96-well Immulon-2 microtiter plates (Dynatech Laboratories, Chantilly, VA, USA) were coated with 100 μl of PBS containing 20 μg/ml of glutathione *S*-transferase (GST)-ADAM8 disintegrin fusion protein or control GST protein and incubated overnight at 4°C. The 96-well plates were blocked with 1% BSA (Calbiochem, San Diego, CA, USA) for 1 h at room temperature. After washing with PBS, 10^5 CHO cells stably expressing α_V, α_9 and/or β_1, β_3, integrin (generously provided by Dr Takada, Y Scripps Research Institute, La Jolla, CA, USA) were added to the wells in 100 μl of DMEM supplemented with 1% BSA and incubated at 37°C for 1 h. Unbound cells were removed by washing with PBS and the remaining cells counted with an inverted microscope. GST protein was used as a negative control. In selected experiments, the GST-ADAM8–coated plates were also pretreated with a blocking antibody to α_9 integrin (clone Y9A2; Chemicon, Temecula, CA, USA) before the CHO cells were added.

OCL formation assays

Mouse bone marrow cultures were performed as previously described.(4) Briefly, nonadherent mouse bone marrow cells from 4–6-week-old $\alpha_9^{+/-}$ mice, 7-day-old $\alpha_9^{+/-}$, or $\alpha_9^{-/-}$ C57BL/6 mice were cultured for 6–9 days in either eight-well chamber slides (Nunc), 48- or 96-well plates in α-MEM containing 10% FCS with $1\alpha,25(OH)_2D_3$ (10^{-9} M), or 10 ng/ml M-CSF, and 50 ng/ml hRANKL. At different times during the culture period, the cells were fixed and stained for TRACP or total RNA was extracted from the cells using RNA-BEE (Tel Test, Friendswood, TX, USA). In selected experiments, bone marrow cells were cultured on sperm whale dentin slices. After 1 week of culture, the dentin slices were stained with hematoxylin, and the number of OCLs was counted. The cells on the dentin slices were removed by rubbing the slices, and the number of resorption pits was scored microscopically.

Human bone marrow cultures were performed as previously described.(2,15) The studies were approved by the Institutional Review Board of the University of Pittsburgh. After obtaining informed consent, 2 ml of bone marrow was aspirated from the posterior superior iliac crest of healthy normal volunteers into a 20-ml syringe containing 1 ml of α-MEM and 1000 U/ml of heparin. The mononuclear cell fraction was obtained by Ficoll-Hypaque density gradient centrifugation, and the mononuclear cells (5×10^6 cells/ml) were collected and incubated in α-MEM containing 20% FCS overnight at 37°C in 100-mm tissue culture plates to deplete adherent cells. Nonadherent bone marrow cells were cultured in 96-well plates in α-MEM containing 20% horse serum in the presence of RANKL (50 ng/ml) and M-CSF (10 ng/ml) or 10^{-8} M $1\alpha,25(OH)_2D_3$. The cultures were fed every 3 days by replacing one half the media, and after 21 days of culture, the cells were fixed with 1% formaldehyde. OCL-like cells were identified by cross-reactivity with the monoclonal antibody 23c6 using a Vectastatin-ABC-AP kit (Vector Laboratories, Burlingame, CA, USA). The 23c6-positive OCLs were scored using an inverted microscope.

In selected experiments, nonadherent mononuclear cells were cultured in methylcellulose culture as described previously(16) to form CFU-GM colonies. In brief, CFU-GM colonies

were formed by culturing 10^5 nonadherent marrow mononuclear cells/ml in 0.3% methylcellulose in α-MEM with 30% FCS in 35-mm tissue culture plates in presence of 100 pg/ml granulocyte-macrophage colony-stimulating factor (GM-CSF) for 7–10 days. The CFU-GM colonies (>40 cells) were morphologically identified by light microscopy and individually collected. CFU-GM–derived cells are highly purified early OCL precursors.(16)

RT-PCR and real-time RT-PCR analysis

Total RNA was extracted from bone marrow cells cultured for 1–7 days using RNA-BEE (Tel Test), and the cDNA was synthesized from 1 μg of total RNA using the SuperScript reverse transcriptase system (Invitrogen, Carlsbad, CA, USA) in a total volume of 20 μl. The resulting cDNA products were subjected to PCR analysis using primers specific for α_9 integrin (5′-CCTAACGTTGCACTGCAACC-3′ sense, 5′-AGCAGAAAAATGAGGATCCCC-3′ antisense; accession no. NM_133721); α_v (5′-AATCTCCAGTGGCCTTACAA-3′ sense, 5′-AGGAAGCAGATGACTTCAGG-3′ antisense; accession no. NM_008402); ADAM8 (5′-ATGCTACTGTCCTGAACCAC-3′ sense, 5′-ACTGAGACGACACACCTCTC-3′; accession no. NM_007403); GAPDH (5′-ACCACAGTCCATGCCATCAC-3′ sense, 5′-TCC-ACCACCCTGTTGCTGTA-3′ antisense; accession no. NM_001001303). The PCR amplification was performed by incubating the sample at 94°C for 30 s, 58°C for 30 s, and 68° C for 1 minute for 20–35 cycles. The PCR products were electrophoresed on a 1.5–2% agarose gel containing ethidium bromide. For real-time RT-PCR analysis, α9 primers were 5′-TCAACATCACAGCACCTGAG-3′ (forward) and 5′-AGCCGTCAGATTGTAGTTCAG-3′ (reverse); for ADAM8, 5′-ATGCTACTGTCCTGAACCAC-3′ (forward) and 5′-TGCTACACCTGCTGAATATCC-3′ (reverse); and for GAPDH, 5′-GCCTTCCGTGTTCCTACC-3′ (forward) and 5′-GCCTGCTTCACCACCTTC-3′ (reverse). The correlation coefficients for each amplification were 0.99 or higher, and the amplicons were visualized on 4% agarose gel as well. A Bio-Rad iCycler and iQ SYBR green supermix were used for the real-time RT-RCR analysis. The running conditions were incubation at 94°C for 2 minutes and 40 cycles of incubation of 94°C for 30 s, 50°C for 30 s, and 72°C for 30 s, with final incubation at 72°C for 7 minutes.

Western blot analysis

Cells were lysed in a buffer containing 1% Triton X-100 in 50 mM Tris-HCl (pH 7.4) containing 150 mM NaCl, 2 mM Na_3VO_4, 100 mM NaF, and protease inhibitors and subjected to Western blot analysis. The protein concentration of the samples was measured using the BioRad Bradford reagent according to the manufacturer's protocol. Protein samples (20 μg) were subjected to electrophoresis, using 8–12% polyacrylamide gels. The proteins were transferred onto nitrocellulose membranes for immunoblot analysis. After blocking with 5% nonfat dry milk or 2% BSA in 150 mM NaCl, 50 mM Tris (pH 7.2), 0.05% Tween 20 (TBST) buffer, the membrane was incubated for 1 h with an anti-$\alpha_9\beta_1$ or β-actin antibodies diluted 1:1000 in 5% non-fat dry milk-TBST. The blots were incubated for 1 h with horseradish peroxidase (HRP)–conjugated goat anti-mouse or anti-rabbit IgG diluted 1:2500 in 5% nonfat dry milk-TBST or 2% BSA and visualized using the ECL system (Amersham, Arlington Heights, IL, USA).

Immunocytochemistry

Cells were fixed with 3.7% formaldehyde for 20 minutes. After being rinsed, cells were blocked with H_2O_2 for 30 minutes and blocked with 2% horse serum for 30 minutes. Cells were incubated overnight with primary antibody at 4°C and for 1 h at room temperature with an HRP-labeled secondary antibody; goat anti-mouse or anti-rabbit IgG (Santa Cruz). For phalloidin-Texas red (Invitrogen) staining, the cells were fixed with 3.7% formaldehyde and per-meabilized with 0.1% Triton-X 100 in PBS before staining. Control staining was performed by replacing the primary antibody with normal mouse IgG. Cell morphology was observed

with an Olympus epi-fluorescence microscope and recorded with a Magnafire digital camera (Optronics), or a Leica TCS-SL confocal microscope system (Leica Microsystems, Weltzlar, Germany) with a ×40 oil (NA 1.25) lens.

μCT Analysis

Fifth lumbar vertebrae of 7-day-old $\alpha_9^{-/-}$ and wildtype littermate mice (five mice of each genotype) were fixed in 3.7% formaldehyde and used for 3D μCT analysis. First, 2D CT horizontal slices of the lumbar were obtained with a Scanco vivaCT40 (Scanco Medical, Bassersdorf, Switzerland). The thickness of slices was 10 μm. 3D images were reconstructed using the software provided by Scanco. The trabecular bone was measured in the tissue area. Parameters analyzed from 3D images included the ratio of trabecular bone volume and total bone volume (TV/BV), trabecular thickness (Tb.Th), trabecular number (Tb.N), and trabecular separation (Tb.Sp). The threshold for the 3D analysis was set at 175.

Histology

The undecalcified fifth lumbar vertebrae of 7-day-old $\alpha_9^{-/-}$ and WT littermate mice ($n = 5$) were sectioned into 4 μm on a cryostat (CryoJane Tape-Transfer System). The sections were fixed in citrate/acetone solution or 3.7% formaldehyde for TRACP staining or H&E staining, respectively. TRACP activity was detected by incubation with a mixture of 0.1 mg/ml naphthol AS-MX phosphate (Sigma), 0.5% *N*,*N*-dimethylformamide, and 0.6 mg/ml fast red AL salt (Sigma) in 0.1 M acetate buffer solution (pH 5.0) at 37°C for 30 minutes. H&E staining was performed using standard procedures. The slides were viewed with a Nikon TE2000 inverted microscope equipped with a Spot 12 bit 1600 × 1200 pixel CCD camera. Histomorphometric analysis was performed using the Fovea Pro Analysis System (Reindeer Graphics, Asheville, NC, USA) according to the American Society of Bone and Mineral Research Histomorphometry Committee.(17)

Data analysis

Data were expressed as mean ± SE. Statistical differences were determined using ANOVA for repeated measures; p values <0.05 were considered to be significant.

RESULTS

Binding of CHO cells expressing integrin $\alpha_v\beta_3$ and $\alpha_9\beta_1$ to a GST-ADAM8 fusion protein

We previously reported that the disintegrin domain of ADAM8 mediated its stimulatory effects on OCL formation.(3) To identify which integrin subunit interacted with ADAM8, we tested the adherence of CHO cells homogenously expressing human integrin $\alpha_V\beta_3$ or $\alpha_9\beta_1$ to plates coated with the disintegrin domain of GST-ADAM8 or control GST protein. CHO cells expressing the integrin $\alpha_9\beta_1$ subunit significantly bound the ADAM8 disintegrin domain, whereas CHO cells expressing integrin $\alpha_v\beta_3$ did not significantly bind to ADAM8 (Fig. 1A). All transformed CHO cells minimally bound the control GST protein (data not shown). To confirm the specificity of the interaction of ADAM8, plates coated with GST-ADAM8 fusion protein were pretreated with an anti-α_9 antibody and the CHO cells transformed with $\alpha_v\beta_3$ or $\alpha_9\beta_1$ cDNA were allowed to attach to the plates. The addition of α_9 antibody completely inhibited the binding of $\alpha_9\beta_1$ to GST-ADAM8 fusion protein (Fig. 1B), but did not alter background binding to $\alpha_v\beta_3$.

α_9 integrin expression on mouse and human OCL precursors

α_9 integrin is expressed in airway epithelial cells, airway and gut smooth muscle, keratinocytes, hepatocytes, and neutrophils, but expression of α_9 on OCLs or their precursors has not been reported. To examine if α_9 integrin is expressed during OCL differentiation, real-time

quantitative RT-PCR analysis for α_9 and ADAM8 mRNA was performed on mouse bone marrow cultures treated with RANKL/M-CSF for 1–7 days of culture. Expression of α_9 mRNA progressively increased during OCL differentiation (Fig. 2A), as did the expression of ADAM8. In addition, the expression levels of α_v were similar between $\alpha_9^{-/-}$ and WT mice (Fig. 2B).

Purified human OCL precursors were tested for α_9 integrin expression. Western blot analysis of lysates from highly purified human OCL precursors showed a 140-kDa α_9 integrin band (Fig. 3A). No band was detected in the control lane. OCL precursors were positively stained (Fig. 3B) by a monoclonal anti-human α_9 antibody. The dark stained area surrounding the cells denoted a positive reaction. Control staining performed without primary antibody showed no staining (data not shown). When highly purified CFU-GM derived and human OCL precursors were treated with RANKL (50 ng/ml) and M-CSF (10 ng/ml) for 7 days, both α_9 and ADAM8 mRNA was expressed (Figs. 3C and 3D) as shown by RT-PCR analysis.

Anti-α_9 antibody inhibits OCL formation

We previously reported that ADAM8 stimulated OCL formation and bone resorption and that an antisense construct to ADAM8 inhibited OCL formation induced by RANKL or 1α,25 $(OH)_2D_3$. (6) To determine if α_9 integrin was involved in OCL formation, we tested the effects of a blocking α_9 antibody on OCL formation in human marrow cultures treated with 1α,25 $(OH)_2D_3$ (10^{-8} M). When human bone marrow cultures were treated with an antibody to α_9 for 3 weeks, OCL formation was reduced significantly (Fig. 4A) at an antibody concentration of 1.0 μg/ml compared with the control mouse IgG (1.0 μg/ml). Addition of 10μg/ml of anti-a_9 antibody did not further inhibit OCL formation (data not shown). Because OCL formation from bone marrow nonadherent cells occurs in the presence of other cells in the culture, we also used purified OCL precursors to test if the α_9 antibody inhibited OCL formation by OCL precursors. Highly purified human CFU-GM–derived cells were treated with RANKL (50 ng/ml) and M-CSF (10 ng/ml) in the presence or absence of anti-α_9 for 3 weeks. Treatment with α_9 antibody significantly decreased OCL formation (Fig. 4B).

OCL formation and the bone histomorphometry of $\alpha_9^{-/-}$ mice

To assess the role of $\alpha_9\beta_1$ in OCL differentiation, we analyzed OCL formation in marrow cultures in $\alpha_9^{-/-}$ mice, because α_9 only forms a heterodimer with the β_1 subunit, and β_1 knockout mice are embryonic lethal. Mice homozygous for a null mutation in α_9 die of chylothorax at 7–10 days after birth.(13) Therefore, nonadherent bone marrow cells from 7-day-old $\alpha_9^{-/-}$ or WT mice were cultured with RANKL (50 ng/ml) and M-CSF (10 ng/ml) for 7 days to induce OCL formation. The cultures were fixed and stained for TRACP. $TRACP^+$ OCLs from $\alpha_9^{-/-}$ mice were smaller compared with WT (Fig. 5A). Approximately 10% of the OCLs present in the $\alpha_9^{-/-}$ cultures appeared normal in size. When bone marrow cells from $\alpha_9^{-/-}$ or WT mice were cultured on dentin slices for 7 days, WT OCLs formed normal numbers of resorption pits and with serpentine-like moving trails. In contrast, $\alpha_9^{-/-}$ OCLs formed dramatically fewer resorption pits (Fig. 5B). Furthermore, the total area resorbed on dentine slices was dramatically decreased when cultured with $\alpha_9^{-/-}$ OCLs (Fig. 5C). In addition, OCLs from $\alpha_9^{-/-}$ mice had decreased bone resorption efficiency per cell, as indicated in Fig. 5D. These data suggest that OCLs from $\alpha_9^{-/-}$ had an impaired bone resorption capacity and that this is not simply caused by decreased numbers of OCLs formed.

Actin ring formation is required for OCL bone resorption. Because $\alpha_9^{-/-}$ OCLs had an impaired bone resorption capacity, we examined actin ring formation in these cells with phalloidin staining. As shown in Fig. 6A, although $\alpha_9^{-/-}$ OCLs could form an actin-ring/podosome belt, they did not form well-defined lamellipodia in contrast to WT OCLs. In addition, some podosomes were loosely scattered around the dense podosome belt in $\alpha_9^{-/-}$ OCLs, as seen by

the enlarged podosome belt at the right of the actin ring. To further evaluate the OCL cytoskeleton, we measured the osteoclast height (the distance between the basolateral membrane facing the bone marrow space and the ruffled border). Osteoclast height has been used as an index of osteoclast polarization.(18) $\alpha_9^{-/-}$ OCLs had a significantly decreased height compared with WT OCLs, suggesting $\alpha_9^{-/-}$ OCLs had impaired polarization (Fig. 6B).

Histological analysis showed that vertebrae from 7-day-old $\alpha_9^{-/-}$ mice had moderately thickened trabecular regions, retained cartilage within vertebral bodies, an odd convex shape, and more abundant trabecular bone in the vertebrae compared with WT littermates (Fig. 7A). 3D reconstruction of the fifth lumbar vertebrae (Fig. 7B) showed denser bone and intervertebral discs in $\alpha_9^{-/-}$ mice compared with WT. There was no difference in OCL numbers or surface between WT and $\alpha_9^{-/-}$ vertebrae (data not shown). Furthermore, 3D μCT analysis of the fifth lumbar vertebrae revealed a modest but significant increase in trabecular bone volume/total tissue volume (WT = 16 ± 1.6%; $\alpha_9^{-/-}$ = 20 ± 4.1%; p =0.04; Fig. 7C), and a tendency of decreased trabecular separation (p =0.06) in $\alpha_9^{-/-}$ mice compared with WT mice.

DISCUSSION

Integrins are matrix receptors that transduce the signals bidirectionally inside-out and outside-in the cell.(19,20) They play a key role in OCL activity by mediating OCL adhesion and regulating cytoskeleton organization.(21,22) OCLs express very high levels of the $\alpha_v\beta_3$ integrin,(23) which regulates osteoclastic bone resorption.(11,24) OCLs also express lower levels of other type integrins, including $\alpha_2\beta_1$, $\alpha_v\beta_1$, $\alpha_v\alpha_5$, and $\alpha_5\beta_1$.(12,25) In this study, we showed that $\alpha_9\beta_1$ integrin is expressed on OCL precursors and mature OCLs and that it interacts with ADAM8. This conclusion is based on our studies that showed that ADAM8 binds $\alpha_9\beta_1$ and not $\alpha_v\beta_3$. ADAM8 lacks an RGD motif; therefore, it is not surprising that it does not bind $\alpha_v\beta_3$. ADAM family members that lack an RGD sequence can bind or $\alpha_9\beta_1$ $\alpha_4\beta_1$ because these integrins have high structural homology. However, we and others have been unable to detect $\alpha_4\beta_1$ integrin on OCL precursors either by PCR or by Western blot analysis.(26)

Time-course studies suggested that ADAM8/$\alpha_9\beta_1$ effects on OCL formation start at the early stage of OCL precursor differentiation. Murine and human OCL precursors expressed $\alpha_9\beta_1$ integrin at a very early stage, and $\alpha_9\beta_1$ integrin and ADAM8 expression increased with subsequent differentiation. The mRNA expression level of both and α_9 ADAM8 was increased significantly over time. These data suggest that the effects of ADAM8 on OCL formation are mediated through interactions with $\alpha_9\beta_1$.(3,27) These results are consistent with our previous time-course studies in which ADAM8 was added at various times during the culture period and was found to act at the later stages of OCL precursor differentiation.(6) Further support for a role for $\alpha_9\beta_1$ in OCL formation are our experiments using an anti-body to α_9, which showed that it significantly inhibited OCL formation induced by $1\alpha,25(OH)_2D_3$ or RANKL and M-CSF.

$\alpha_9\beta_1$ did not seem to play a critical role in OCL formation because OCL numbers in vitro were only decreased by 30%, but rather its primary effects were on OCL function. OCLs formed in marrow cultures from $\alpha_9^{-/-}$ mice were small and contracted. Although $\alpha_9^{-/-}$ OCLs can form actin rings, they did not form lamellipodia, indicating impaired OCL mobility. In support of this conclusion, WT OCL formed a serpentine-like bone-resorption trail, whereas $\alpha_9^{-/-}$ OCLs formed only dot-like resorption pits. Furthermore, $\alpha_9^{-/-}$ OCLs had impaired polarization as indicated by the decreased osteoclast height. These defects resulted in a decreased bone resorption capacity for the $\alpha_9^{-/-}$ OCLs. This is despite the fact that $\alpha_9^{-/-}$ OCLs express normal amounts of $\alpha_v\beta_3$. In preliminary experiments, we found that activation of by ADAM8 induced phosphorylation of α_9 paxillin in OCL precursors. These data are consistent with previous reports of the α_9 signaling pathway in other cell types.(28) Multiple signaling pathways have

been implicated in the induction of OCL formation. Because of cross-talk between these signaling pathways, it is likely that more than one signaling pathway is involved in α_9 regulation of osteoclastogenesis.

Histologic analysis of bones from $\alpha_9^{-/-}$ mice further suggests that $\alpha_9^{-/-}$ OCLs are dysfunctional in vivo. Bones from 7-day-old $\alpha_9^{-/-}$ mice showed decreased resorption of cartilage and thickened trabeculae and had a significant increase in the BV/TV ratio on μCT analysis. However, trabecular number was not significantly reduced. This is not surprising because we could only examined mice at 7 days of age. The lack of a definitive bone phenotype at this very early age is similar to results published for mice lacking the β_3 integrin, which do not develop osteosclerosis until ~6 months of age.(11) Yamamoto et al.(26) have also suggested a role for α_9 in bone resorption and examined the molecular mechanisms of osteopontin (OPN) action in rheumatoid arthritis (RA), using collagen-induced arthritis (CIA) as an in vivo model. Levels of thrombin-cleaved OPN (OPN-T) are increased in synovial fluid and serum from patients with RA. OPN-T expresses a cryptic epitope, SLAYGLR, which is chemotactic for monocytes expressing α_9 and α_4 integrins. Monocytes from animals with CIA had increased expression of integrin mRNA. When these animals were α_9 treated with an antibody to SLAYGLR, M5, there was less proliferation of the synovium and a marked decrease in bone erosion. These data are consistent with our findings that plays an important role in OCL function and $\alpha_9\beta_1$ suggest that may contribute to the increased OCL $\alpha_9\beta_1$ activity in inflammatory bone loss.

Acknowledgements

This study was support by NIH Grants RO1-AR41336, AG12951, and AR47700.

References

1. Roodman GD. Cell biology of the osteoclast. Exp Hematol 1999;27:1229–1241. [PubMed: 10428500]
2. Kurihara N, Chenu C, Miller M, Civin C, Roodman GD. Identification of committed mononuclear precursors for osteoclast-like cells formed in long-term human marrow cultures. Endocrinology 1990;126:2733–2741. [PubMed: 2184023]
3. Choi SJ, Devlin RD, Reddy SV, Chung H, Boyce BF, Roodman GD. Identification of human asparaginyl endopeptidase (legumain) as an autocrine inhibitor of osteoclast formation and bone resorption. J Biol Chem 1999;274:27747–27753. [PubMed: 10488118]
4. Oba Y, Chung HY, Roodman GD, Choi SJ. Eosinophil chemotactic Factor-L (ECF-L): A novel osteoclast stimulating factor. J Bone Miner Res 2003;18:1332–1341. [PubMed: 12854845]
5. Huovila APJ, Almeia EA, White JM. ADAMs and cell fusion. Curr Opin Cell Biol 1996;8:692–699. [PubMed: 8939659]
6. Choi SJ, Han JH, Roodman GD. ADAM8: A novel osteoclast stimulating factor. J Bone Miner Res 2001;16:814–822. [PubMed: 11341326]
7. Wolfsberg TG, Primakoff P, Myles DG, White JM. ADAM, novel family of membrane proteins containing a disintegrin and metalloprotease domain: Multipotential functions in cell-cell and cell-matrix interaction. J Cell Biol 1995;131:275–278. [PubMed: 7593158]
8. Wu E, Croucher PI, McKie N. Expression of members of the novel membrane linked metalloproteinase family ADAM in cells derived from a range of hematological malignancies. Biochem Biophys Res Commun 1997;235:437–442. [PubMed: 9199213]
9. Bohm BB, Aigner T, Gehrsitz A, Blobel CP, Kalden JR, Burkhardt H. Upregulation of MDC15 (metargidin) messenger RNA in human osteoarthritic cartilage. Arthritis Rheum 1999;42:1946–1950. [PubMed: 10513811]
10. Yoshiyama K, Higuchi Y, Kataoka M, Matsuura K, Yamamoto S. CD 156 (human ADAM8): Expression, primary amino acid sequence, and gene location. Genomics 1997;41:56–62. [PubMed: 9126482]

11. McHugh KP, Hodivala-Dilke K, Zheng MH, Namba N, Lam J, Novack D, Feng X, Ross FP, Hynes RO, Teitelbaum SL. Mice lacking β3 integrins are osteosclerotic because of dysfunctional osteoclasts. J Clin Invest 2000;105:433–440. [PubMed: 10683372]
12. Hughes DE, Salter DM, Dedhar S, Simpson R. Integrin expression in human bone. J Bone Miner Res 1993;8:527–533. [PubMed: 8511980]
13. Huang XZ, Wu JF, Ferrando R, Lee JH, Wang YL, Farese RV Jr, Sheppard D. Fatal bilateral chylothorax in mice lacking the integrin alpha9beta1. Mol Cell Biol 2000;20:5208–5215. [PubMed: 10866676]
14. Eto K, Puzon-McLaughlin W, Sheppard D, Sehara-Fujisawa A, Zhang XP, Takada Y. RGD-independent binding of integrin alpha9beta1 to the ADAM-12 and -15 disintegrin domains mediates cell-cell interaction. J Biol Chem 2000;275:34922–34930. [PubMed: 10944520]
15. Kurihara N, Reddy SV, Menaa C, Anderson D, Roodman GD. Osteoclasts expressing the measles virus nucleocapsid gene display a pagetic phenotype. J Clin Invest 2000;105:607–614. [PubMed: 10712432]
16. Menaa C, Kurihara N, Roodman GD. CFU-GM-derived cells form osteoclasts at a very high efficiency. Biochem Biophys Res Commun 2000;267:943–946. [PubMed: 10673396]
17. Parfitt AM, Drezner MK, Glorieux FH, Kanis JA, Malluche H, Meunier PJ, Ott SM, Recker RR. Bone histomorphometry: Standardization of nomenclature, symbols, and units. Report of the ASBMR Histomorphometry Nomenclature Committee. J Bone Miner Res 1987;2:595–610. [PubMed: 3455637]
18. Faccio R, Teitelbaum SL, Fujikawa K, Chappel J, Zallone A, Tybulewicx VL, Ross FP, Swat W. Vav3 regulates osteoclast function and bone mass. Nat Med 2005;11:284–290. [PubMed: 15711558]
19. Hynes RO. Integrins: Versatility, modulation and signaling in cell adhesion. Cell 1992;69:11–25. [PubMed: 1555235]
20. Hynes RO. Integrins: Bidirectional, allosteric signaling machines. Cell 2002;110:673–687. [PubMed: 12297042]
21. Faccio R, Grano M, Colucci S, Zallone AZ, Quaranta V, Pelletier AJ. Activation of alphav beta3 integrin on human osteoclast-like cells stimulates adhesion and migration in response to osteopontin. Biochem Biophys Res Commun 1998;249:522–525. [PubMed: 9712729]
22. Feng X, Novack DV, Faccio R, Ory DS, Aya K, Boyer MI, McHugh KP, Ross FP, Teitelbaum SL. A Glanzmann's mutation in beta 3 integrin specifically impairs osteoclast function. J Clin Invest 2001;107:1137–1144. [PubMed: 11342577]
23. Horton MA. The alpha v beta 3 integrin "vitronectin receptor". Int J Biochem Cell Biol 1997;29:721–725. [PubMed: 9251239]
24. Hodivala-Dilke KM, McHugh KP, Tsakiris DA, Rayburn H, Crowley D, Ullman-Cullere M, Ross FP, Coller BS, Teitelbaum S, Hynes RO. Beta3-integrin-deficient mice are a model for Glanzmann thrombasthenia showing placental defects and reduced survival. J Clin Invest 1999;103:229–238. [PubMed: 9916135]
25. Duong LT, Lakkakorpi P, Nakamura I, Rodan GA. Integrins and signaling in osteoclast function. Matrix Biol 2000;19:97–105. [PubMed: 10842093]
26. Yamamoto N, Sakai F, Kon S, Morimoto J, Kimura C, Yamazaki H, Okazaki I, Seki N, Fujii T, Uede T. Essential role of the cryptic epitope SLAYGLR within osteopontin in a murine model of rheumatoid arthritis. J Clin Invest 2003;112:181–188. [PubMed: 12865407]
27. Biskobing DM, Fan X, Rubin J. Characterization of MCSF-induced proliferation and subsequent osteoclast formation in murine marrow culture. J Bone Miner Res 1995;10:1025–1032. [PubMed: 7484277]
28. Young BA, Taooka Y, Liu S, Askins KJ, Yokosaki Y, Thomas SM, Sheppard D. The cytoplasmic domain of the integrin alpha9 subunit requires the adaptor protein paxillin to inhibit cell spreading but promotes cell migration in a paxillin-independent manner. Mol Biol Cell 2001;12:3214–3225. [PubMed: 11598204]

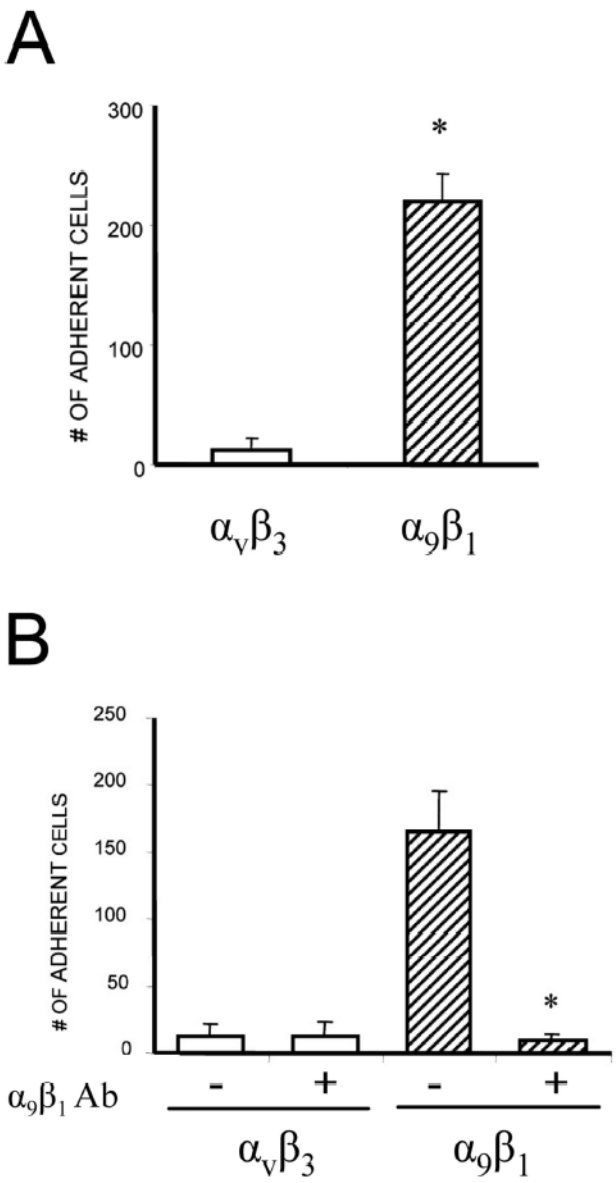

FIG 1.

Adhesive capacity of CHO cells expressing heterodimeric integrin subunits. Adhesion of CHO cells stably expressing $\alpha_9\beta_1$ or $\alpha_v\beta_3$ integrin to the disintegrin domain of ADAM8. (A) Adhesion was measured by counting the number of adherent cells with an inverted microscope. Adhesion capacity of CHO cells expressing $\alpha_9\beta_1$ integrin to the disintegrin domain of ADAM8 was significantly enhanced compared with integrin, $\alpha_v\beta_3$. (B) Effects of anti-$\alpha_9\beta_1$ antibody on CHO cell adhesion. In addition to being coated with the GST-ADAM8 fusion protein, the culture plates were pretreated with a blocking antibody against $\alpha_9\beta_1$ (10 μg/ml). The adhesion of stably expressing $\alpha_9\beta_1$ CHO cells to the culture plates was significantly decreased. Similar results were found in three independent experiments. Results from one typical experiment are shown as mean ± SE (*$p < 0.05$).

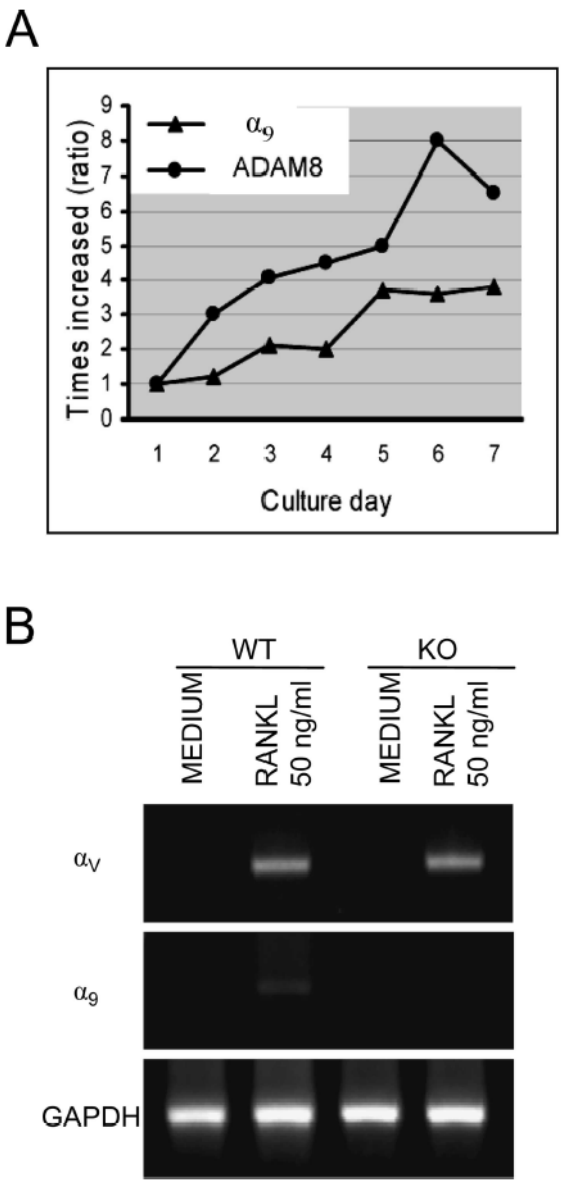

FIG 2.

Expression of α_9 during mouse bone marrow OCL differentiation. (A) Mouse bone marrow nonadherent cells were treated with RANKL (50 ng/ml) and M-CSF (10 ng/ml) for varying time intervals. The cells were harvested at different time-points as indicated and analyzed for α_9 and ADAM8 mRNA expression by real-time RT-PCR using specific primers. (B) Non-adherent bone marrow cells from $\alpha_9^{-/-}$ and WT mice were incubated with factors as indicated for 3 days. The α_v integrin expression levels were analyzed by RT-PCR. Similar results were found in three independent experiments. Results from one typical experiment are shown.

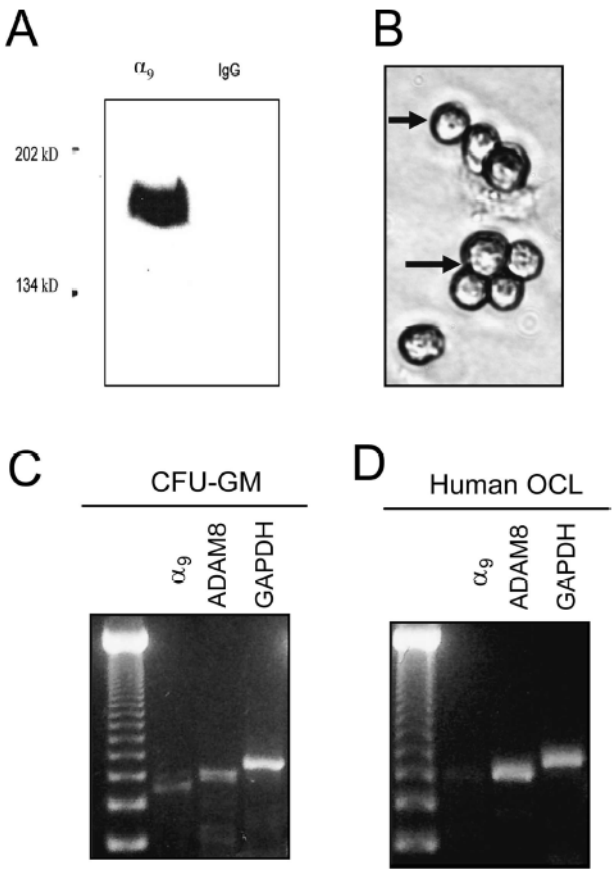

FIG 3.

Expression of α_9 integrin on human osteoclasts and precursors. (A) Western blot analysis of human CFU-GM derived cell lysates with monoclonal anti-human α_9 antibody. A 140-kDa α_9 integrin band was detected in lysates from highly purified OCL precursors. No band was detected in the control lane. (B) Immunocytochemistry for α_9 expression on osteoclast precursors (CFU-GM–derived cells) treated with $1\alpha,25(OH)_2D_3(10^{-8}$ M) for 5 days. RT-PCR analysis for α_9 and ADAM8 expression in (C) CFU-GM–derived cells and (D) OCLs formed from human CFU-GM–derived OCL precursors induced with 50 ng/ml RANKL and 10 ng/ml M-CSF in liquid cultures.

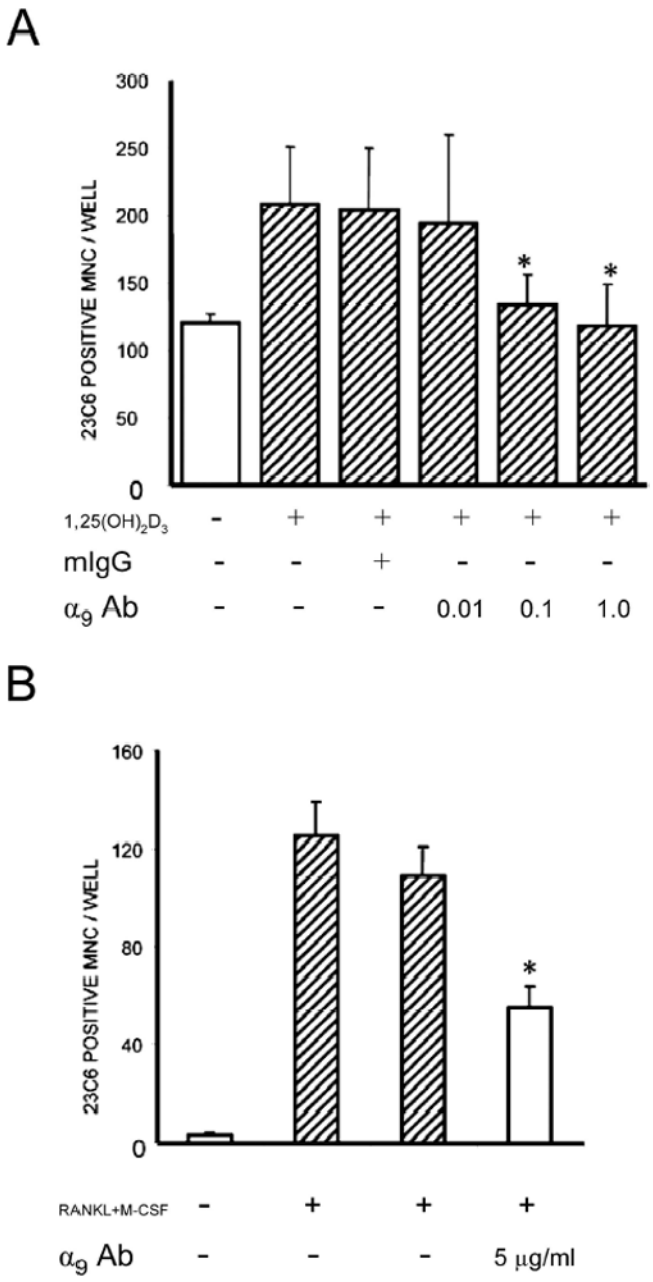

FIG 4.

Anti-α_9 integrin inhibits OCL formation by human CFU-GM–derived cells. (A) Human bone marrow cells stimulated with $1\alpha,25(OH)_2D_3$ (10^{-8} M) were treated with varying concentrations of anti-α_9 antibody (μg/ml as indicated in the figure) and cultured for 3 weeks. (B) CFU-GM–derived cells were treated with RANKL (50 ng/ml) and M-CSF (10 ng/ml) in the presence or absence of anti-α_9 for 3 weeks. At the end of the culture period, cells were fixed and stained with the 23C6 monoclonal antibody that identifies the osteoclast vitronectin receptor. $23c6^+$ multinucleated cells containing three or more nuclei per cell were scored as OCLs. Mouse IgG was used as a control. Results represent the mean ± SE for the number of OCL formed (*$p < 0.05$) for a typical experiment. Similar results were found in three independent experiments.

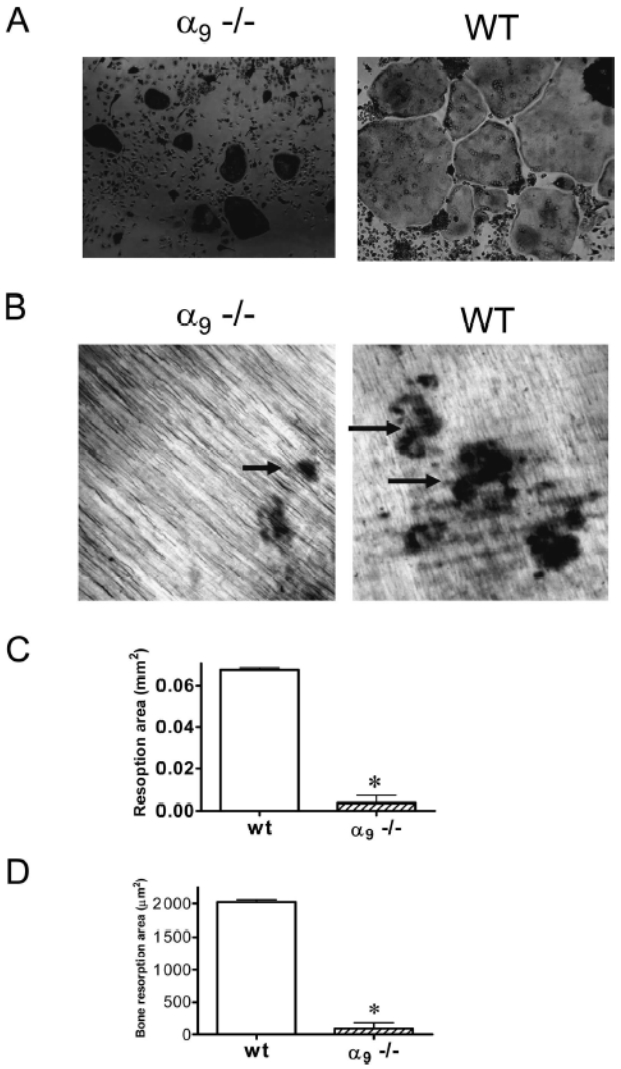

FIG 5.

OCL formation and bone resorption in bone marrow cultures from $\alpha_9^{-/-}$ mice. Bone marrow cells from 7-day-old $\alpha_9^{-/-}$ or WT mice were cultured with RANKL (50 ng/ml) and M-CSF (10 ng/ml) for 7 days. The cultures were fixed and stained for TRACP. (A) OCLs formed from $\alpha_9^{-/-}$ were smaller and more contracted than those in WT cultures. After 7 days, the cells were removed from dentin. The resorption pits formed on dentin were visualized by light microscopy after staining with hematoxylin. (B) $\alpha_9^{-/-}$ OCLs formed dramatically fewer resorption pits. In contrast, WT OCLs formed numerous and serpentine-like resorption pits. In addition, OCL resorption capacity was determined by measuring (C) total bone resorption areas and (D) the average resorption area per OCL. Magnification: ×10. Similar results were found in three independent experiments. Results from one typical experiment are shown as mean ± SE (*p < 0.05).

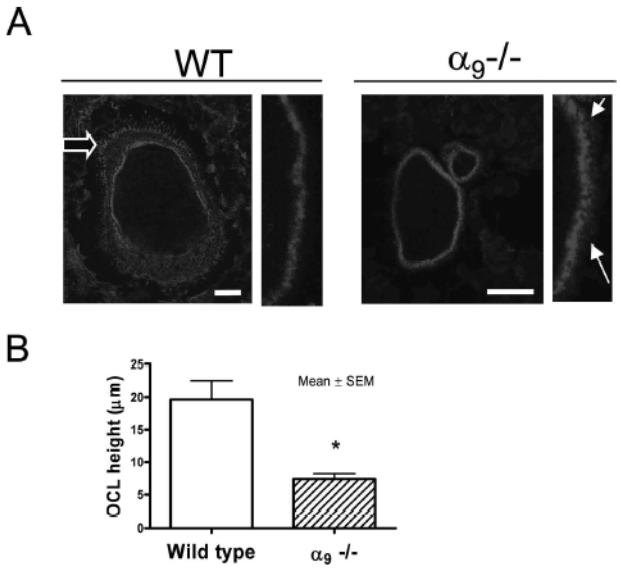

FIG 6.

Cytoskeleton dysfunction and actin-ring deformation in $\alpha_9^{-/-}$ OCLs. (A) OCLs formed from $\alpha_9^{-/-}$ and WT marrow cultures were stained with Texas-red-phalloidin (magnification, ×10; scale: 25 μm). **(A)** Left: actin-ring formation in WT and $\alpha_9^{-/-}$ OCL; fine structure of the podosome belt is shown at higher power. Open arrow shows the lamellipodium. Solid arrows show the loosely distributed podosomes at the edge of actin-ring. (B) Osteoclast height in WT and $\alpha_9^{-/-}$ OCLs. Similar results were found in three independent experiments. Results from one typical experiment are shown.

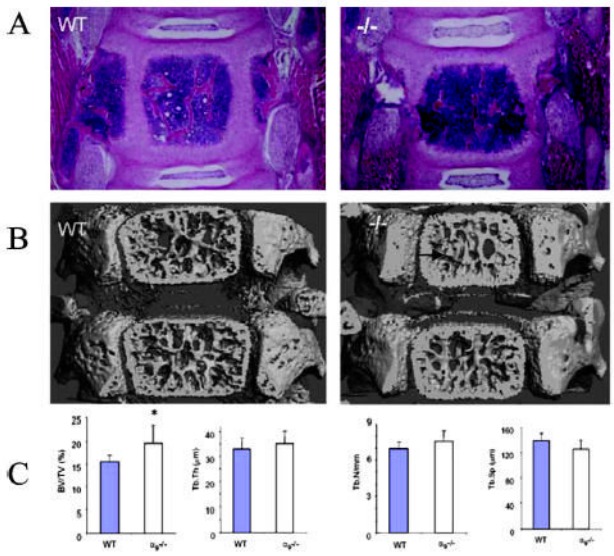

FIG 7.

Histologic and μCT analysis of $\alpha_9^{-/-}$ mice vertebrae. (A) Coronal section of a fifth vertebrae stained with H&E staining outlined thickened trabeculae in $\alpha_9^{-/-}$ mice compared with WT (magnification, ×4). (B) μCT reconstructed fifth lumbar vertebrae images of 7-day-old WT mice. (C) Bone morphometric analyses of the fifth vertebrae from μCT indices of the fifth lumbar vertebrae bone showed a significant increase of the ratio of trabecular bone volume to total bone volume (BV/TV) in $\alpha_9^{-/-}$ mice compared with WT. BV/TV, bone volume/total volume; Tb.Th, trabecular bone thickness; Tb.N, trabecular bone number; Tb.Sp, trabecular bone separation. Mean ± SE for five mice/group are shown. *$p < 0.05$ by Student *t*-test.